J Comp Physiol A (1994) 174:633–642

Journal of Comparative Physiology A Sensory, Neural, and Behavioral Physiology

Waveform generation in *Rhamphichthys rostratus* (L.) (Teleostei, Gymnotiformes)

The electric organ and its spatiotemporal activation pattern

A. Caputi, O. Macadar, O. Trujillo-Cenóz

Divisions of Comparative Neuroanatomy and Neurophysiology, Instituto de Investigaciones Biológicas "Clemente Estable", Av. Italia 3318, CP11600, Montevideo, Uruguay

Accepted: 11 October 1993

Abstract. *Rhamphichthys rostratus* (L.) emits brief pulses (2 ms) repeated very regularly at 50 Hz. The electric organ shows a heterogeneous distribution of the electrocyte tubes and the occurrence of three electrocyte types (caudally innervated, rostrally innervated and marginally-caudally innervated). In the sub-opercular region the electric organ consists of a pair of tubes containing only caudally innervated electrocytes. At the abdominal region the EO consists of three pairs of tubes. Each pair contains one of the described electrocyte types. The number of electrocyte tubes increases toward the tail to reach nine or ten pairs in the most caudal segments. In the intermediate region most tubes contain doubly innervated electrocytes except the ventral pair that contains caudally innervated electrocytes. The caudal 25% contains exclusively caudally innervated electrocytes. The electric organ discharge consists of five wave components (V1 to V5). Electrophysiological data are consistent with the hypothesis that V1 results from the activity of the rostral faces of rostrally innervated electrocytes. V2 results from the activities of rostral faces of marginally-caudally innervated electrocytes while V3 results from the activities of caudal faces of most electrocytes. Curarization experiments demonstrated that V4 and V5 result from action potential invasion and are not directly elicited by neural activity.

Key words: Electrogeneration – Electric organ – Electrocytes – Electric fish – Rhamphichthyidae

Abbreviations: AEN1, anterior electromotor nerve 1; AEN2, anterior electromotor nerve 2; BMB, boraxic methylene blue; CIE, caudally innervated electrocytes; EMF, electromotive force; EO, electric organ; EOD, electric organ discharge; *I*, current amplitude; MCIE, marginally-caudally innervated electrocytes; MT, medial tubes; PEN, posterior electromotor nerve; R_i, internal impedance; RIE, rostrally innervated electrocytes; Rl, load resistor; SAT, short abdominal tubes; *V*, voltage amplitude

Correspondence to: A. Caputi

Introduction

The diverse group of South American electric fish (Order Gymnotiformes) includes approximately 60 species usually separated in six families (Mago-Leccia 1978). These fish are able to generate species-specific EODs differing in amplitude, repetition rate and waveform. Adapted to live in a variety of ecological niches they exhibit complex behaviors that have been explored in detail only in a few species (Hopkins 1983, 1988).

Most electrogenic systems show a common pattern of organization: the EO consists of several tubes lying dorsal to the anal fin musculature and extending along the fish body. With the exception of the Apteronotidae, in which the adult EO is formed by modified spinal electromotor axons, in all other taxa the EO tubes contain electrogenic units – electrocytes – of myogenic origin. Variations involving both the morphology and the electrophysiological properties of the electrocytes have been described in different species (Bennett 1971; Bass 1986). Investigations dealing with the EOs and EODs of gymnotids have been mainly focused on species belonging to five families (Sternopygidae, Hypopomidae, Apteronotidae, Gymnotidae and Electrophoridae), while information concerning the remaining family (Rhamphichthyidae) is limited to behavioral aspects (Lissmann and Schwassmann 1965; Bennett 1971; Schwassmann 1976; Bass 1986).

As stressed by Bullock (1984, 1986, 1993), proper understanding of the evolution and functional organization of neural systems requires studies dealing with many species covering the major branches of each taxonomic group.

The present paper is concerned with the morphology of the EO and the EOD characteristics of *Rhamphichthys rostratus* (L.) (family Rhamphichthyidae). Technical procedures developed during previous investigations on *Gymnotus carapo* (Trujillo-Cenóz et al. 1984; Lorenzo et al. 1988; Trujillo-Cenóz and Echagüe 1989; Macadar et al. 1989; Caputi et al. 1989; Caputi et al. 1993) have provided the basis for this investigation.

R. rostratus is a pulse fish with a multiphasic, highly regular discharge. As previously found in *G. carapo* the EOD waveform exhibits a spatio-temporal pattern determined by the EO structural organization.

Material and methods

Fish. Four large *R. rostratus* (54, 65, 68 and 70 cm) were captured at night in the gate for migrating fish of Salto Grande hydroelectric plant (Uruguay river, west limit of Uruguay state). This species has been described for this biogeographical zone (von Ihering 1907; Ellis 1913) and the taxonomic identification was made using Ellis'-key. Taking into account that the taxonomy and phyletic relationships of the Gymnotiformes are under revision (Mago-Leccia 1978; Fink and Fink 1981; Gayet and Meunier 1991) the species identification should be considered tentative. However, von Ihering (1907, pp. 279 original in Portuguese) advanced that: "It seems very probable that with abundant material from diverse regions, it will be verified that the alleged species *(R. rostratus marmoratus; R. rostratus reinhardti)* lack support even as sub-species; in the case to be grouped in a single species this must be named *Rhamphichthys rostratus (L.)*".

One of the collected specimens died during manipulations in the gate. It was immediately fixed by immersion in 10% formaldehyde and used for gross-anatomy studies. The other three animals were kept alive in a large aquarium and used for both electrophysiological experimentation and finer anatomical analysis. Fish were treated with special care to avoid injuries that might impair survival. After obtaining the desired functional data, the animals were fixed by perfusion as described in the following paragraphs. All morphological and functional findings have been referred to percentage of fish length, with the tip of the head 0% and the tip of the tail 100%.

Anatomical procedures. Deeply anesthetized fish (1 mg ethomidate/1 ml water) were perfused through the heart with 5% paraformaldehyde dissolved in 0.1 mol · l^{-1} phosphate buffer. Before passing the fixative fluid, blood was removed from the vascular bed with a fish-adapted saline solution. Both the washing solution and the fixative were propelled with a peristaltic pump. Cross sections of the fish body were cut at different rostro-caudal levels to explore the distribution of the electrogenic tissue. For this purpose the scales were removed and the vertebral column was cut with a fine saw; soft tissues were sectioned with a very sharp knife. Each section (approximately 2 mm thick) was cleared with glycerol and mounted between two pieces of flat glass. The more slender tail portions were cut with a vibratome (in these cases sections were 400 µm thick). Large sections were projected with the aid of a photographic enlarger and the outlines of both the fish body and the EO were drawn on paper sheets. The vibratome sections were observed under a light microscope and the outlines of the relevant structures were drawn with the aid of a camera lucida.

The different tubes composing the EO were dissected out and immersed in buffered osmium tetroxide (1% OsO_4 in 0.1 mol · l^{-1} phosphate buffer). Osmicated tubes were cleared with glycerol and studied under the microscope. In other instances the tubes were disrupted and single electrocytes were isolated to be observed and photographed under the microscope. Isolated electrocytes were also dehydrated and epoxy-resin embedded. Semithin sections (1–2 µm thick) were cut with a LKB Ultrotome and stained with BMB. Series of ultrathin sections were mounted on Formvar-coated grids and doubly stained with uranyl acetate and lead citrate. The fine structure of the electrocytes was analyzed with a transmission electron microscope at different magnifications.

Electrophysiological procedures. The EOD was characterized using the same methods applied to study *G. carapo* (Caputi et al. 1989, 1993). Briefly, the EMF and R_i of the whole fish body were cal-

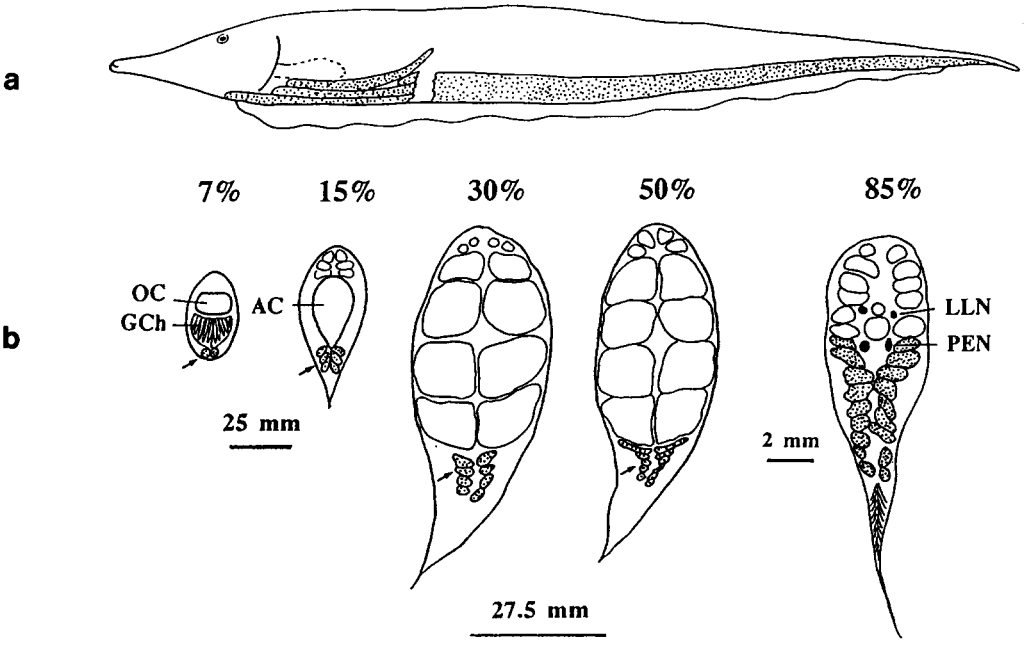

Fig. 1 a A schematized lateral view of the EO (*stippled*) of *R. rostratus*. The EO is represented as discontinuous and for the sake of clarity natural proportions have not been maintained. Individual electrocyte tubes are shown only in the sub-opercular and abdominal portions, while in the remainder intermediate and caudal portions the EO has been represented as a whole (the *break* shows the point at which the individual tubes are no longer represented). **b** Five transverse sections depicting the number of electrocyte tubes at different percentages of the fish length (the tip of the head is considered to be 0% and the tip of the tail 100%). The electrocyte tubes appear *stippled*; in the drawings showing 7%, 15%, 30% and 50% of the fish length, the *arrows* indicate the EO location. The *open areas* correspond to the main muscular masses. Note that only in the drawing representing a cross section at 85% of the fish length are the lateral line nerves (*LLN*) and the posterior electromotor nerves (*PEN*) shown. *OC* oral cavity; *GCh* gills chamber; *AC* abdominal cavity

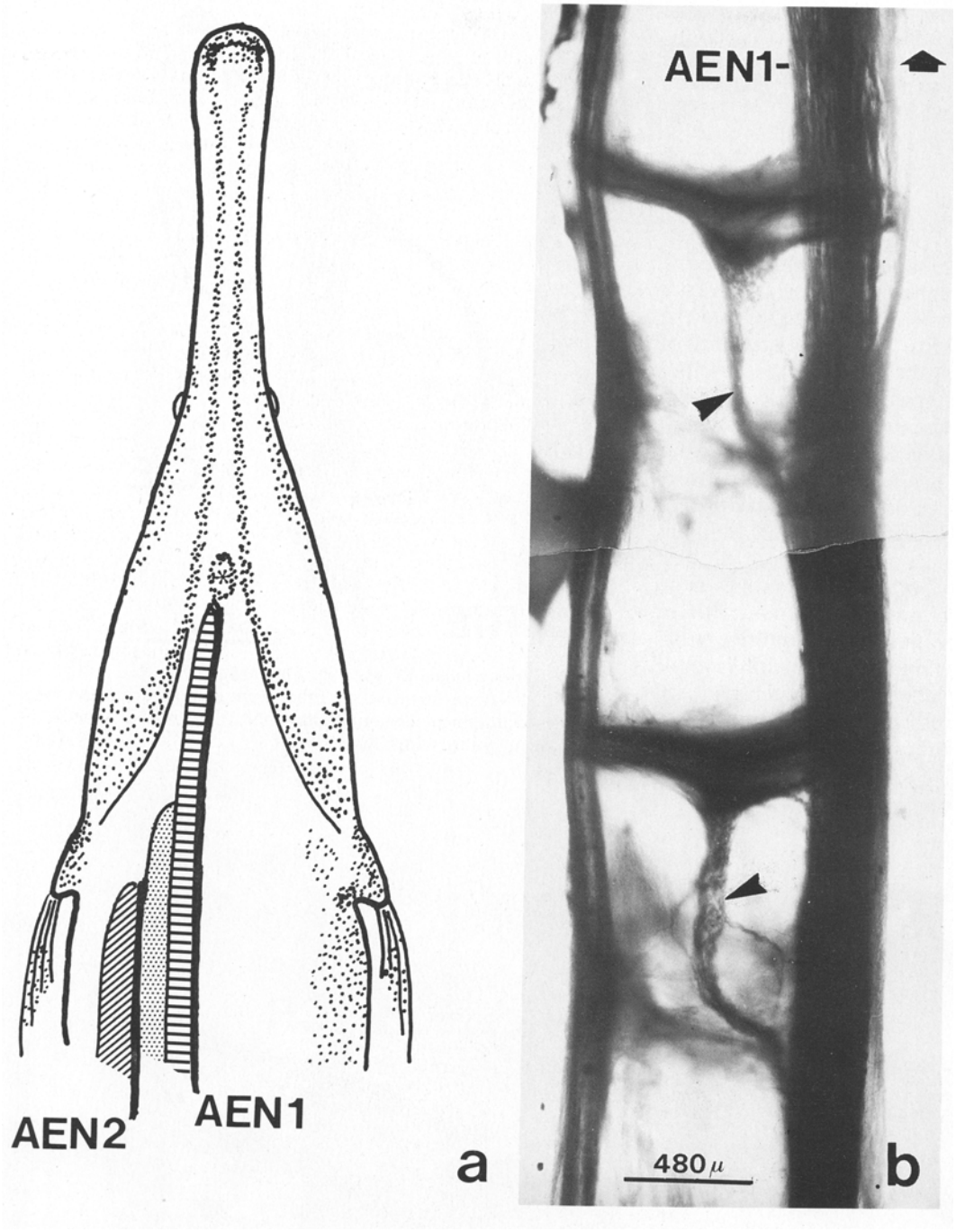

Fig. 2. a Semischematic representation of the rostral portion of *R. rostratus* (ventral view). The *left side* of the picture shows the three electrocyte tubes and the two anterior electromotor nerves (*AEN1* and *AEN2*). The medial tube *(horizontal shading)* contains only CIEs. The more lateral tube *(diagonal shading)* only contains RIEs, while the intermediate tube *(stippled)* contains MCIEs. **b** Low power microphotograph showing two CIEs contained in the medial tube. The *arrowheads* indicate the axon bundles arising from the AEN1. The *thick short arrow* points rostrally. × 40

culated measuring voltage drop and current across known Rls. For this purpose fish were suspended in air and tap water was circulated through the gills.

Two electrodes, one placed in the mouth and the other in the tip of the tail, were connected by known Rls. V and I amplitudes were measured on the oscilloscope screen. Since V was found to be a linear function of I ($V = \mathrm{EMF} - R_i \cdot I$), the ordinate intercept and the slope of the line were considered as good estimators of the EMF and the R_i, respectively. The locally generated discharge was recorded in air with two electrodes placed 2% of the fish length apart (approximately 1 cm) and sequentially moved from head to tail.

The spatio-temporal pattern of the discharge was analyzed by means of the "multiple air-gap technique". The EMF generated by each one of the four quarters of the fish body were simultaneously recorded using the device described in Caputi et al. (1993). The fish were placed in a four-compartment Plexiglass box (see Fig. 10) in such a way that its body passed through successive conductive (2% of the fish body length) and isolating media (23%). Each conductive compartment was connected to a high-input impedance unity-gain non-inverting buffer amplifier, with their outputs connected to differential amplifiers. The current generated by each studied portion produces a voltage drop across the input resistance of the recording amplifier. This resistance was several order of magnitude larger than the fish's R_i. In such conditions the currents are negligible and the recorded voltages are equivalent to the EMFs. This procedure avoids load sharing and permits one to obtain the values of each portion independently of neighboring regions. Amplified signals were either recorded on a pulse-code modulation video cassette recorder or directly digitized (50 kHz sampling frequency) and stored in a computer.

Bipolar field potentials were recorded using a differential amplifier while the fish was resting in the aquarium. In these experi-

ments the electrodes were placed 1 cm apart and the rostral electrode was connected to the non-inverting input of the amplifier.

Partial curarization (*d*-tubocurarine, 1.5 $\mu g \cdot g^{-1}$) was used as in Caputi et al. (1989, 1993) to complement anatomical-functional data concerning the mechanisms subserving V4 and V5.

Results

Anatomical organization of the EO

The EO extends all along the body of the fish forming an anatomical unit. However there are regional variations involving the number of electrocyte tubes and the electrocyte innervation patterns. The gross anatomy of the EO will be described first disregarding the distribution of dissimilar electrocyte types. The EO is composed, at different percentages of the fish length, of different number of electrocyte tubes (Fig. 1). In the sub-opercular region (sample at 7% of the fish length) the EO consists of one tube at each side of the midline. The number of tubes increases dramatically toward the tail. Samples obtained from the abdominal portion (15% of the fish length) showed three bilateral tubes while samples from the intermediate portion (obtained at 30% and 50% of the fish length) showed respectively, four and five tubes at each side of the midline. At the caudal portion (sample obtained at 85% of the fish length) nine or ten bilateral tubes occupy most of the cross section (occasionally an asymmetric distribution of tubes was found).

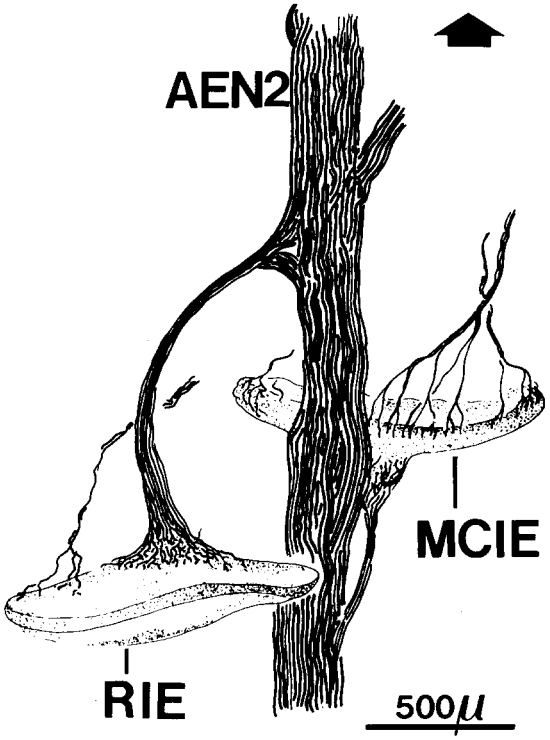

Fig. 3. Camera lucida drawing showing at the *left* a RIE and at the *right* a MCIE. In this case the tubes were disrupted but the electrocytes maintained their nerve attachments to AEN2. The *thick short arrow* points rostrally. × 40

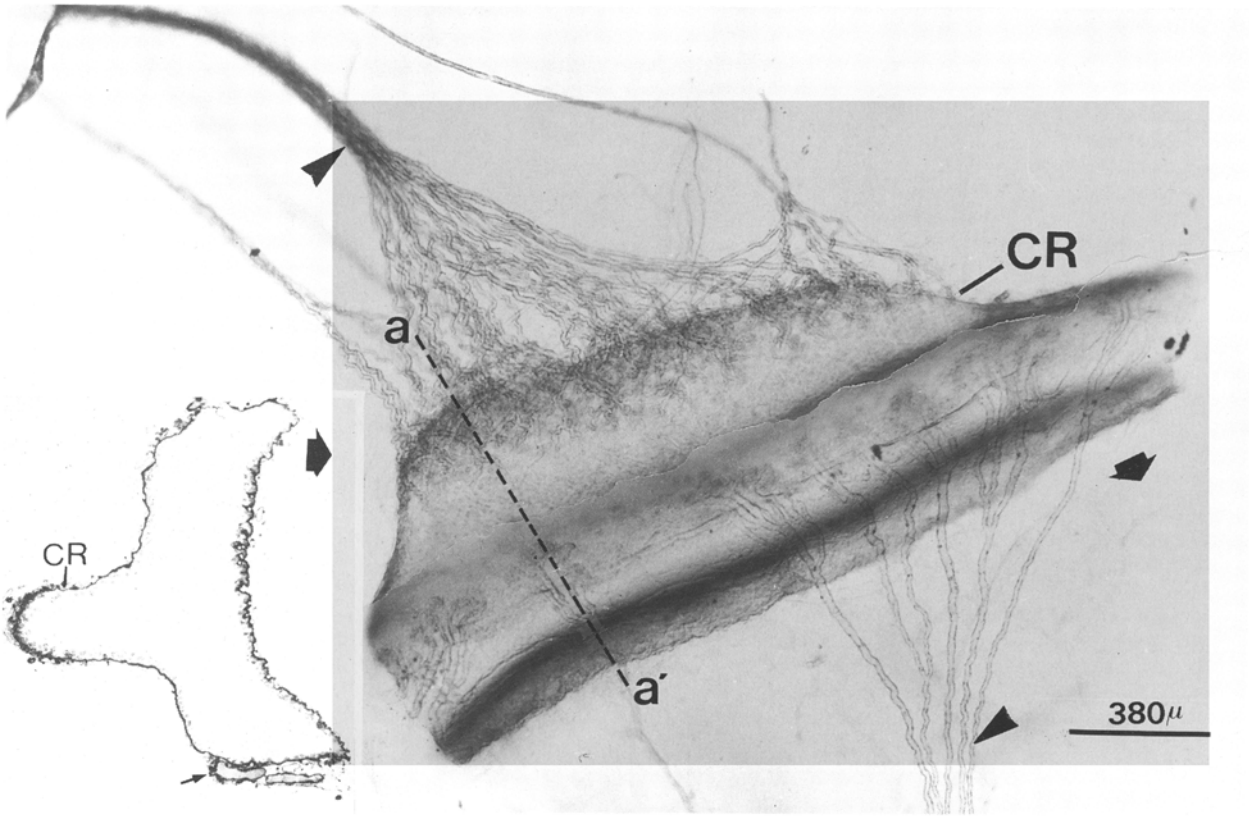

Fig. 4. Photomontage covering two focal planes of an osmium-stained MCIE. The *two arrowheads* indicate the axon bundles terminating in the caudal ridge (*CR*) and in the electrocyte margin. The *inset* shows a semi-thin BMB stained section; the section level is indicated in the photomontage (*dotted line a–a'*). The *small arrow* indicates one thick axon contributing to the marginal innervation. In both microphotographs (shown at the same magnification) the *thick short arrows* point rostrally. × 50

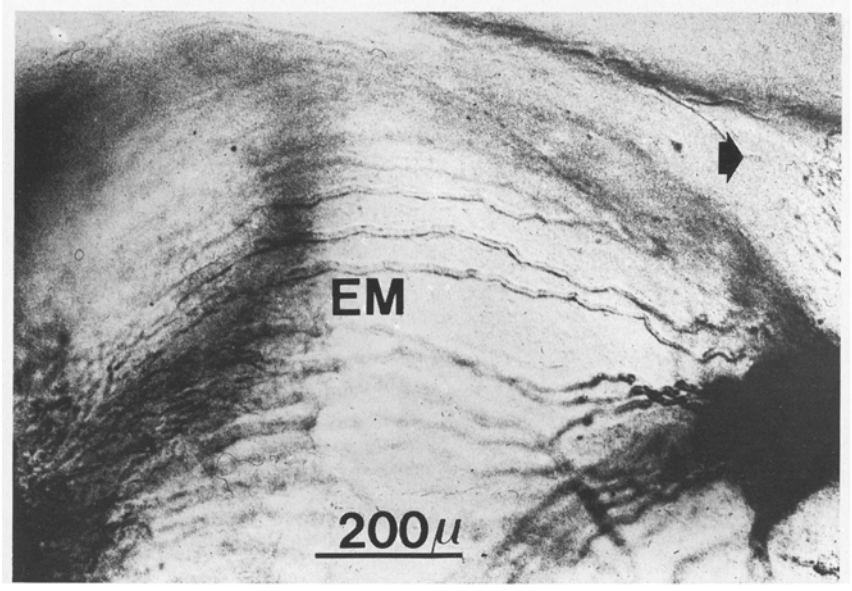

Fig. 5. View of the marginal zone of an osmicated MCIE at a higher magnification. Note the regular arrangement of the preterminal axons that form a palisade perpendicular to the electrocyte margin (*EM*). The *thick short arrow* points rostrally. × 100

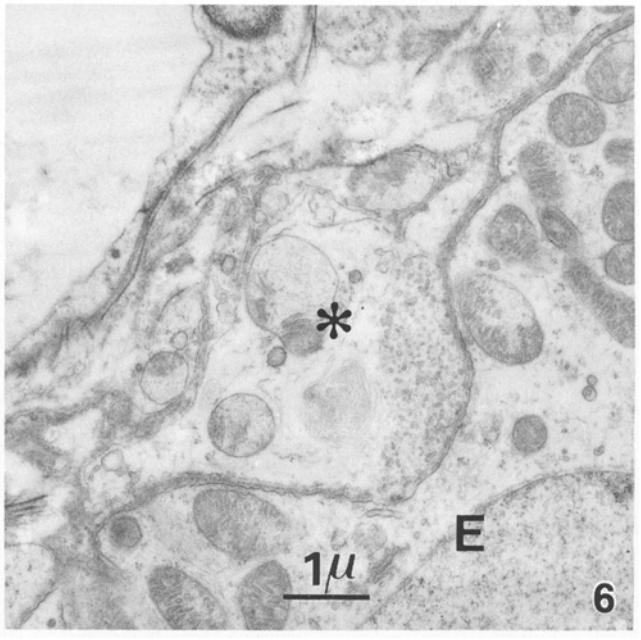

Fig. 6. Electronmicrograph showing a synaptic junction on the marginal zone of a MCIE. Note that the nerve terminal *(asterisk)* lies in a shallow depression of the electrocyte (*E*) plasma membrane. × 11000

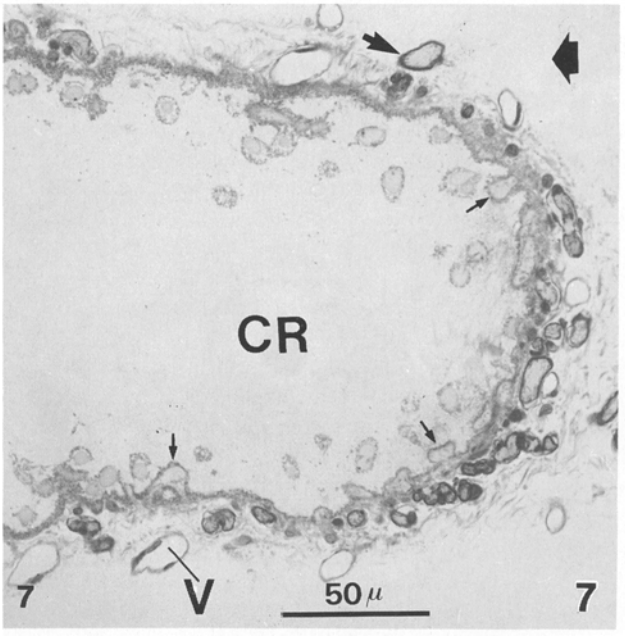

Fig. 7. Semi-thin section passing through the caudal ridge (*CR*) of a MCIE. The *small arrows* indicate nerve terminals deeply encased in the electrocyte plasma membrane. The *medium size arrow* indicates a preterminal axon; *V* blood vessel. The *thick short arrow* points rostrally. × 380

In this species there are three types of electrocytes with different patterns of innervation: RIEs, CIEs and doubly innervated electrocytes. The latter receive innervation on both their caudal and marginal faces (MCIE). The peculiar morphology of these doubly innervated electrocytes will be treated in more detail below.

As described when dealing with the gross anatomy of the EO, the sub-opercular region contains a pair of MT arranged one at each side of the midline. The MTs are particularly long, extending from the 7% to 100% of the fish length; they contain CIEs. The three pairs of tubes found in the abdominal region contain different kinds of electrocytes: in addition to the MTs containing CIEs, there are at this level a pair of SATs composed of RIEs and a pair of intermediate tubes containing MCIEs (Fig. 2). The intermediate EO region (from 30% to 70% of the fish length) consists of several tubes (see above) containing MCIEs and CIEs. The most ventral tubes are the MTs found in the sub-opercular and abdominal regions and contain CIEs; the other additional tubes (three to eight at each side of the midline) contain MCIEs. The caudal region of the EO (70% to 100% of the fish length) consists of nine or ten bilateral tubes containing exclusively CIEs. In summary in the most rostral sub-opercular portion of

the EO only a small number of CIEs occur; the abdominal region contains three electrocyte types (CIEs, RIEs and MCIEs); in the intermediate region only two electrocyte types are found (a majority of MCIEs and a smaller number of CIEs); finally the caudal region only contains a large number of CIEs.

As shown in Figs. 2 and 3, RIEs and CIEs exhibit a similar, conventional electrocyte morphology: they are disk-like structures with only one innervated face. MCIEs, however, are complex and deserve a more detailed description. Each MCIE has a concave rostral surface and a convex caudal surface bearing a large ridge-like projection (Fig. 4). Nerve terminals were found concentrated on the caudal ridge and also forming a palisade on the electrocyte margin. The marginal innervation derives from nerve fibers running in a rostrocaudal direction. These thick (20 μm) but lightly myelinated axons lie regularly arranged all around the electrocyte margin. Closer inspection shows that the nerve fibers surpass the limits of the rostral surface and actually terminate on the marginal surface, or even on the rind of the caudal surface (Fig. 5). Synaptic junctions on the marginal zone are not apparent on BMB sections but their presence was confirmed by means of electron microscope procedures. They occur in shallow depressions of the plasma membrane (Fig. 6). Conversely, synapses on the caudal ridge are easily observed in BMB stained sections; they are characterized by infoldings of the postsynaptic membranes in which the nerve terminals are deeply encased (Fig. 7). In this respect caudal synapses of *Rhamphichthys* electrocytes are similar to those observed in *Gymnotus* electrocytes. In the sub-opercular region there is a pair of AEN1s that provide the nerve branches innervating the caudal faces of the CIEs contained in the MTs. These nerves lie closely apposed to the MT sheaths. At the level of the opercular aperture a pair of AEN2s is added. They run between the intermediate tubes and the SATs. In the abdominal region, branches arising from the AEN2 innervate the caudal faces of CIEs and the rostral faces of the RIEs. In the intermediate and caudal portions a pair of well-developed PENs are found similar to those described in *Gymnotus* (Trujillo-Cenóz et al. 1989).

The spatio-temporal pattern of the EOD

Rhamphichthys rostratus emits brief pulses (2.5 ms duration) at a very constant firing rate (50 ± 0.2 Hz, 23 °C, Fig. 8A). The electrical behavior was quite similar to that

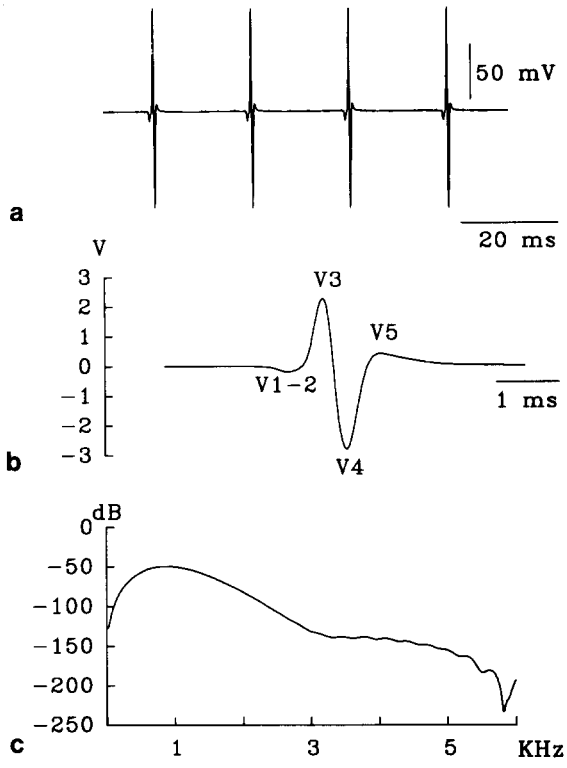

Fig. 8. a Four EODs of *R. rostratus* recorded head-to-tail in water. **b** EMF of a single EOD with its different wave components. **c** Power spectral density of a single EOD (dB referred to the total power).

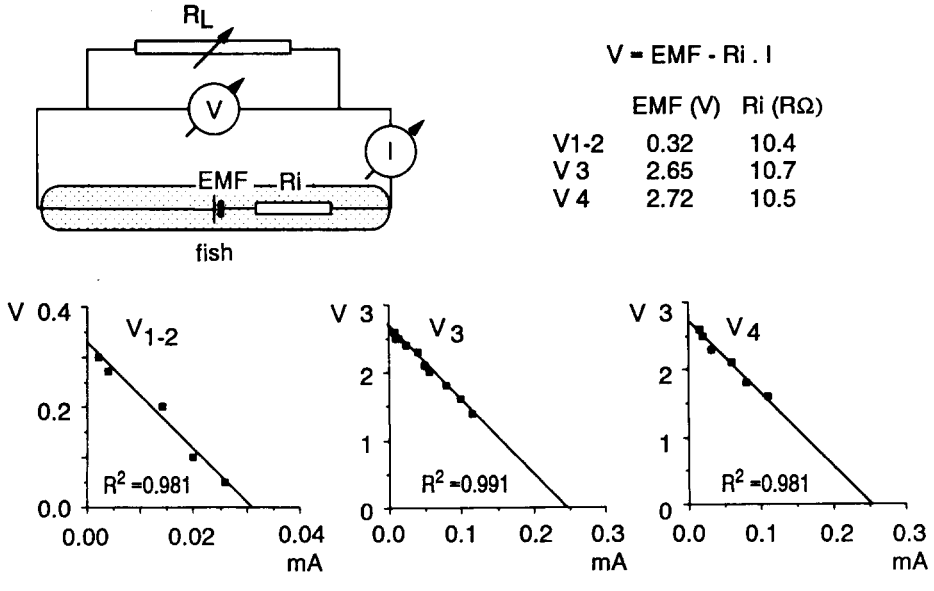

Fig. 9. Sketch of the circuit used to measure V and I generated by the fish in the air-gap condition *(upper left.)*. Plots correspond to the main EOD deflections (V1–2, V3, V4) of the EOD. Each plot shows the relationship between I and V obtained with different load resistances (R_L). The EMF is the ordinate intercept; the R_i is the slope of the line. The resulting values are shown at the *upper right*

described by Kramer et al. (1981) in an undetermined species of the same genus.

The EOD shows four main deflections (head to tail records) here referred to as the V1–2 complex (see following paragraphs), V3, V4 and V5 (Fig. 8B). The power spectral density of a single EOD has a peak at approximately 1 kHz and spreads between 10 Hz and 5 kHz (Fig. 8C).

The EOD wave components have dissimilar EMF amplitudes and dissimilar spatial origins. As shown in Fig. 9, the V1–2 complex is ten times smaller than V3 and V4. The amplitude of V5 is similar to that exhibited by the V1–2 complex. The Ri is about 10.5 kΩ for all wave components. Thus, the maximum power delivered to the load (0.6 mW) occurs when the resistance is about 10 kΩ [theorem of maximal transference of energy, Donaldson (1958)]. This value is similar to the resistance measured between two electrodes immersed in fresh water 50 cm apart. Figure 10 illustrates the spatial distribution of the different EOD wave components: the spatial domain of the V1–2 complex extends from 10 to 75% of the fish body; V3 is generated almost all along the fish (5–100%), while V4 and V5 arise from the caudal 50%. The amplitude of all wave components increases monotonically in a rostro-caudal direction along its spatial domain. As shown in Fig. 10, the peaks of the EOD wave components, recorded from different body portions are not synchronous. For any given wave component the peak at caudal level is delayed with respect to the peak at more rostral levels. This phenomenon can be described as a head-to-tail wave that travels at a mean speed of 2 km · s^{-1}.

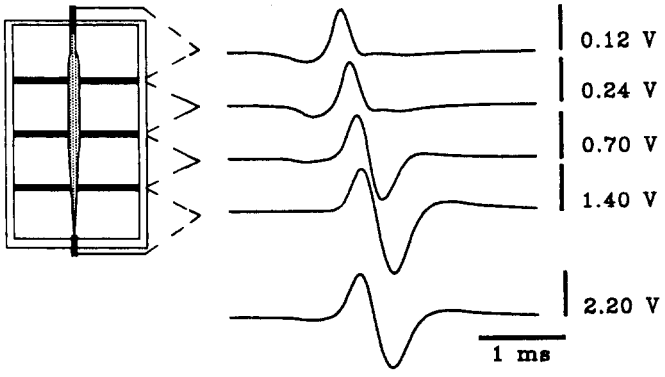

Fig. 10. Spatiotemporal pattern of EMF along the fish body. The four upper traces correspond to successive fish body quarters as recorded in the four gap chamber schematized at the *left*. This procedure avoids load sharing and permits one to obtain the EMF values of each portion independently of neighboring regions. The *lower trace* corresponds to the head-to-tail EOD

Anatomical-functional correlation

In topological correspondence with the anatomical organization four functional portions were identified. Figure 11 shows a summarized view of the anatomical-functional organization of the EO of *R. rostratus* combining electrocyte-type distribution (represented by different shades) and four air-gap (2% fish length-width) recordings. Single-air-gap recordings were sequentially obtained all along the fish length and four representative examples corresponding to the four anatomical regions are shown. The EOD recorded from the opercular region only shows V3. As described in the anatomical section, at this level the EO contains exclusively CIEs.

The air gap studies (Fig. 11) and the rostro-caudal series of bipolar field potentials obtained close to the fish (Fig. 12) revealed that the V1–2 complex consists of two wave components with overlapped spatial and time domains. There are variations in the EOD waveform when air gap and bipolar field potentials are compared. This results from the different load applied to the EO. In the air gap there is no load, whereas in water a complex distributed impedance loads the generator. Wave component amplitudes and peak times depend not only on the fish electrical parameters (local EMF, tissue resistance and skin resistance) but also on the loading media (water resistance, border conditions, etc.). Field poten-

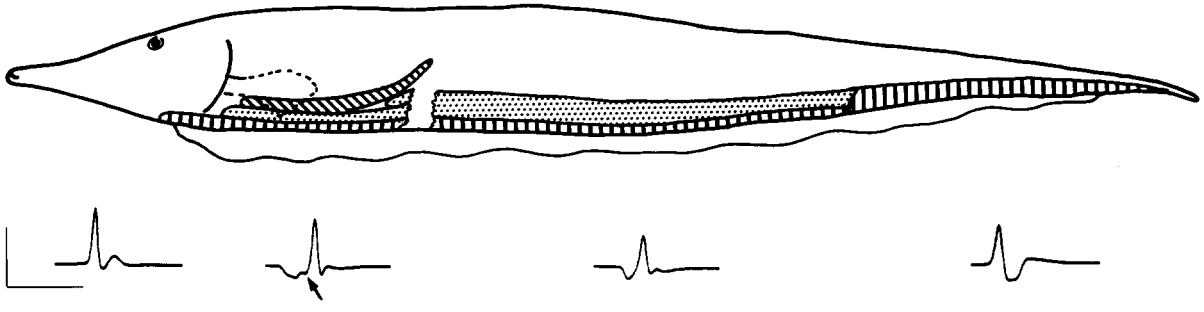

Fig. 11. This semi-schematic drawing correlates different EO portions with samples of the regional EODs (air-gap recordings from 1-cm portions at 10, 20, 60 and 85%). It also illustrates the distribution of the different electrocyte types along the EO (RIEs *diagonal shading;* MCIEs *stippled;* CIEs *vertical shading*). Recordings at 10%, where the EO contains only CIEs, show a monophasic head-positive deflection followed by a small ripple. At the abdominal level, where the three types of electrocytes occur, the V1–2 complex appears *(arrow)*. In the intermediate region (lacking RIEs) the regional EOD lacks V1 while V2 becomes relatively larger. At 85%, where the EO is composed of a large population of small CIEs, the regional EOD shows a single neurally elicited wave (V3) followed by the non-neurally elicited components (V4–V5). Information concerning individual tubes is only provided for the rostral portion (note that the EO has been represented as discontinuous and that the natural proportions have been not maintained). In the intermediate region all tubes containing MCIEs are represented as a whole; in the caudal 25% all tubes contain CIEs and are also represented as a whole. *Vertical calibration bar* corresponds to 25, 50, 150 and 250 mV, respectively. *Horizontal calibration bar:* 3 ms

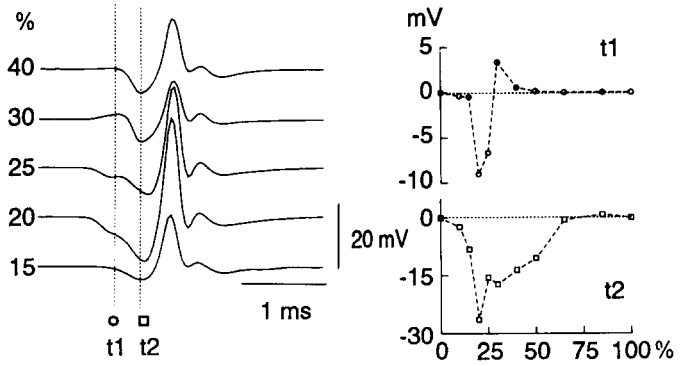

Fig. 12. Field potentials recorded in water facilitated identification of the two wave components of the V1–2 complex. V1 and V2 have overlapping temporal and spatial domains. The traces at the left are successive bipolar recordings (between 15 and 40% of the fish length) of the EOD in water. Plots at the *right* show voltage values obtained at T1 *(circles)* and T2 *(squares)* versus percentage of fish length. V1 originates between 15 and 25% *(upper plot)* while V2 originates between 10 and 75% *(lower plot)*

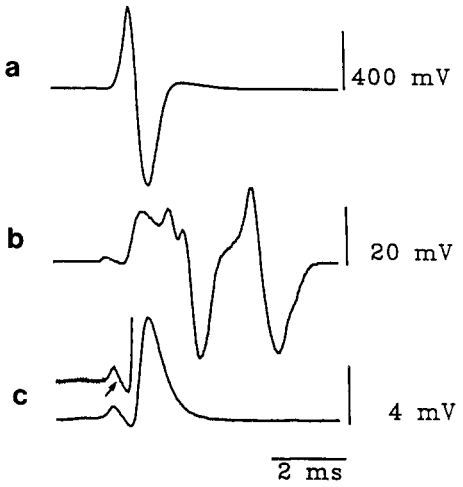

Fig. 13. a–c. Curare dramatically diminished V3 and abolished V4 and V5: **a** control EOD; **b** and **c** curarized animal. After a period characterized by variable patterns of desorganization (example in **b**), the EOD became stabilized, small and monophasic (**c**). The biphasic peripheral nerve activity *(arrow)* remained unchanged. To compare this activity in the same fish before and during curarization, an equally magnified control recording (*inset* in **c**), is included

tials taken close to the fish may be interpreted as the effect through the media of the summated currents that flow between the electrode locations. In the absence of other sources these currents are generated by the EO discharge. Therefore, such records were used only as a qualitative index of the activity of the EO. The place where the amplitude of each wave component (V1 or V2) diminishes indicates the place where the transcutaneal currents change direction. The reversal points indicate the place where transcutaneal current flows attain their maxima and are good indicators of the limits of the generators. The reversal points were close to the caudal limit of the spatial domains of RIEs and MCIEs and also close to the caudal limit of the spatial domains of V1 and V2 (recorded in the air-gap).

The earliest wave component (V1) occurs exclusively at the abdominal region (the region in which RIEs occur), whereas the spatial domain of the other wave component (V2) extends from 10% to 75% of the fish body (the region containing MCIEs). As in the sub-opercular region, V3 results from the activation of the caudal faces of most electrocytes.

Anatomical data have revealed that the tail region of the EO is composed, as in *G. carapo*, of a quite homogeneous population of CIEs. In the latter species V4 is the consequence of the activation of rostral non-innervated faces. A similar situation occurs in *R. rostratus*. The activation of rostral non-innervated faces should arise from action currents spreading from the caudally innervated faces. This hypothesis was tested by recording the EOD of the caudal 10% in partially curarized fish. The temporal evolution of the D-tubocurarine effect was characterized by describing the two stages represented in Fig. 13. The initial stage showed a disorganization of the EOD accompanied by a reduction in its amplitude. The disorganized EOD consisted of an early positive deflection followed by multiple positive-negative discharges that varied in number and amplitude in the course of time. In the second stage, the EOD remnant became stabilized. Curare dramatically diminished V3 and abolished V4 and V5. The EOD remained as a positive deflection resembling in shape and time-course and end-plate potential. Figure 13 also shows a small biphasic (1 mV) deflection (arrow) that did not change in amplitude or shape and may correspond – as demonstrated in *G. carapo* (Caputi et al. 1993) – to the activity of the PEN and its branches. Control and curarized animals showed the same delay between nerve and electrocyte activity.

Discussion

Investigations on the functional organization of the electrogenic system can be based on two complementary strategies: a) the detailed study of a single species concentrating efforts to cover different levels of analysis from behavioral to cellular events, and b) the initiation of comparative studies including less known species and families. The second approach allows one to identify general evolutionary traits and variations from the general structural and functional pattern (Bullock 1984, 1986, 1993).

The idea that the electrocyte innervation pattern is important for determining the EOD waveform was introduced by Bennett and Grundfest (1959) in their pioneer studies on *G. carapo*. More recently we advanced the hypothesis that waveform generation may be dependent upon the electrocyte innervation characteristics, the properties of the neuroelectrocyte junctions and the size and spatial distribution of electrocytes along the EO (Caputi et al. 1989; Macadar 1993). This hypothesis was confirmed by means of single electrocyte recordings (Macadar et al. 1989). The present study dealing with the poorly known *Rhamphichthys* has revealed the occurrence of three types of electrocytes (CIE, RIE and MCIE) with different innervation patterns. Within the conceptual

framework developed in our previous studies the spatial distribution of these three electrocyte types have been related with the different wave components of the EOD.

The EOD of *R. rostratus* consists of four main deflections. A detailed analysis of the first head negative deflection (V1–2 complex) has revealed that it actually consists of two wave components. However, the striking topological correspondence between the spatial domains of these wave components and the distribution of the different electrocyte types suggested that V1 may originate from the activities of the abdominal RIEs while V2 may originate from the more widely distributed MCIEs. V3 probably originates by the activation of the caudal faces of most electrocytes. It is important to emphasize that at the opercular region where only CIEs occur the regional EOD only shows V3 followed by small ripples not elicited by neural command (they were abolished by curare). Since V4 and V5 were abolished by curare it has been inferred that they are not directly elicited by neural command. Moreover, curarization experiments revealed that peripheral nerve activity occurs before V3. Neither in normal condition nor in curarized animals were signs of nerve activity preceding V4 or V5. Previous investigations on *G. carapo* (Caputi et al. 1989; Macadar 1993) revealed that the last EOD wave component (V4) is not neurally elicited: it originates by the invasion of rostrally innervated faces by action potentials triggered on the caudal faces. Likely, V4 and V5 of *Rhamphichthys* have been interpreted as the successive invasion of action potentials previously originated at opposite electrocyte faces. This kind of reverberating phenomena have been occasionally observed in *G. carapo* under experimental conditions (Caputi et al. 1993). In the tail region electrocyte size diminishes while electrocyte density increases. Both features may favor electrotonic activation of electrocyte membranes by outward currents generated in the opposite faces of the same and neighbor electrocytes.

With respect to the progressive delay of the occurrence of the V3 peak along the EO, the same feature was reported in *G. carapo* (Caputi et al. 1993), and in *Electrophorus* by Coates et al. (1940) and Albe-Fessard and Martins-Ferreira (1953). It can be interpreted as a fast excitation wave travelling along the EO. Even though accurate calculation of the wave speed is difficult, it should range between 700 and 2000 $m \cdot s^{-1}$ (when it is assumed that the peak of most rostral V3 coincides with the V2 peak a lower speed is obtained; when it is assumed that V3 peak is not affected by its summation with V2 a high speed is obtained). In no case are these values compatible with nerve conduction velocities (Macadar 1993). Other neural mechanisms, as those proposed by Bennett (1971) and described by Lorenzo et al. (1990) in *G. carapo*, should also occur in *Rhamphichthys*. Figure 11 shows the summarized view of the EO organization of *R. rostratus*, including the corresponding regional EOD waveforms.

The occurrence of doubly innervated electrocytes has been reported only in *G. carapo* (Szabo 1960, 1961; Trujillo-Cenóz et al. 1984), but the present findings indicate that they also occur in another taxon. In the case of *Rhamphichthys* these electrocytes show the following distinctive features: a) the nerve fibers arriving from the rostral side form a regular palisade all over the electrocyte margin; b) synaptic junctions occur on the marginal membrane; c) the caudal face of each MCIE bears a large ridge receiving most of the caudal innervation. Anatomical-functional correlations suggested that MCIEs may be the electrogenic units that give origin to V2 and also contributes to the genesis of V3. As it occurs in *G. carapo* the neural activation of caudal faces may generate V3. Concerning the mechanism subserving V2 there are evidences indicating that it does not result from action potential invasion from caudal faces (V2 occurs before V3). It should be noted that the amplitude of V2 is ten times smaller than V4 in the region of the organ where mainly MCIEs occur (50–75% of the fish length). This feature indicates that not all the electrogenic capability of rostral faces of MCIEs is involved in V2 generation. However, the existence of a highly organized neural palisade on MCIE margin may indicate that such regular arrangement of nerve terminals is involved in the generation of V2. It is an open question whether V2 results from summation of peripheral neural activities (as occur in Apteronotidae), from the graded activation of rostral faces (as occur in lateral abdominal electrocytes of *G. carapo*), or by the combination of both mechanisms. Electrophysiological recordings at the cellular level are required to explore the membrane mechanisms supporting V2 generation.

Acknowledgements. We thank Dr. D. Lorenzo for his comments and useful suggestions. This investigation has been partially supported by: The European Economic Community (Contracts No. CI1*–CT92–0085; CI1*CT901–9861) and the Comisión Sectorial de Investigación Científica de la Universidad de la República.

References

Albe-Fessard D, Martins-Ferreira H (1953) Rôle de la commande nerveuse dans la synchronization du fonctionnement des éléments de l'organe électrique de gymnote, *Electrophorus electricus* L. J Physiol (Paris) 45:533–546

Bass AH (1986) Electric organs revisited. Evolution of a vertebrate communication and orientation organ. In: Bullock TH, Heiligenberg W (eds) Electroreception. Wiley, New York Chistester Brisbane Toronto Singapore, pp 13–70

Bennett MVL (1971) Electroreception. In: Hoar WS, Randall DJ (eds) Fish physiology, vol 5. Academic Press, New York, pp 493–574

Bennett MVL, Grundfest H (1959) Electrophysiology of electric organ in *Gymnotus carapo*. J Gen Physiol 42:1067–1104

Bullock TH (1984) Understanding brains by comparing taxa. Perspect Biol Med 27:510–524

Bullock TH (1986) Significance of findings on electroreception for general neurobiology. In: Bullock TH, Heiligenberg W (eds) Electroreception. Wiley, New York Chistester Brisbane Toronto Singapore, pp 651–672

Bullock TH (1993) How are more complex brains different? One view and agenda for comparative neurobiology. Brain Behav Evol 41:88–96

Caputi A, Macadar O, Trujillo-Cenóz O (1989) Waveform generation in *Gymnotus carapo*. III. Analysis of the fish body as an electric source. J Comp Physiol A 165:361–370

Caputi A, Silva A, Macadar O (1993) Electric organ activation in *Gymnotus carapo*: spinal origin and peripheral mechanisms. J Comp Physiol A 173:227–232

Coates CW, Cox RT, Rosemblith WA, Brown MB (1940) Propagation of the electric impulse along the organs of the electric eel, *Electrophorus electricus* (Linnaeus). Zoologica 25:249–256

Donaldson PEK (1958) Electronic apparatus for biological research. Butterworth, London

Ellis MM (1913) The gymnotoid eels of tropical America. Mem Carnegie Mus 6:109–195

Fink SV, Fink W (1981) Interrelationships of the ostariophysan fishes (Teleostei). Zool J Linn Soc 72:297–353

Gayet M, Meunier J (1991) Première découverte de Gymnotiformes fossiles (Pisces, Ostariophysi) dans le Miocène supérieur de Bolivie. C R Acad Sci Paris 313:471–476

Hopkins CD (1983) Function and mechanisms in electroreception. In: Northcutt RG, Davis RE (eds) Fish neurobiology, vol 1. Ann Arbor Univ of Michigan Press, pp 215–259

Hopkins CD (1988) Neuroethology of electric communication. Annu Rev Neurosci 11:497–535

Ihering R von (1907) Os peices de agua doce do Brazil. Rev Mus Paulista 7:258–336

Kramer B, Tautz J, Markl H (1981) The electric organ discharge sound response in weakly electric fish. J Comp Physiol 143:435–441

Lissmann HW, Schwassmann HO (1965) Activity rhythm of an electric fish *Gymnorhamphichthys hypostomus*. Z Vergl Physiol 51:153–171

Lorenzo D, Velluti JC, Macadar O (1988) Electrophysiological properties of abdominal electrocytes in the weakly electric fish *Gymnotus carapo*. J Comp Physiol A 162:141–144

Lorenzo D, Sierra F, Silva A, Macadar O (1990) Spinal mechanisms of electric organ discharge synchronization in *Gymnotus carapo*. J Comp Physiol A 167:447–452

Macadar O (1993) Motor control of waveform generation in *Gymnotus carapo*. J Comp Physiol A 173:728–729

Macadar O, Lorenzo D, Velluti JC (1989) Waveform generation of the electric organ discharge in *Gymnotus carapo*. II. Electrophysiological properties of single electrocytes. J Comp Physiol A 165:353–360

Mago-Leccia (1978) Los peces de la familia sternopygidae de Venezuela. Acta Cient Venez 29:1–89

Schwassmann HO (1976) Ecology and taxonomic status of different geographic populations of *Gymnorhamphichthys hypostomus* Ellis (Pisces, Cypriniformes, Gymnotoidei). Biotropica 8:25–40

Szabo T (1960) Quelques observations sur l'innervation de l'organe électrique de *Gymnotus carapo*. Arch Anat Microsc Morphol Exp 49:89–92

Szabo T (1961) Les organes électriques de *Gymnotus carapo*. Proc K Ned Akad Wet 64:584–586

Trujillo-Cenóz O, Echagüe JA (1989) Waveform generation of the electric organ discharge in *Gymnotus carapo*. I. Morphology and innervation of the electric organ. J. Comp Physiol A 165:343–351

Trujillo-Cenóz O, Echagüe JA, Macadar O (1984) Innervation pattern and electric organ discharge waveform in *Gymnotus carapo*. J Neurobiol 15:273–281